Per. Mineral. (2000), *69*, 1, 63-78

PERIODICO di MINERALOGIA
established in 1930

An International Journal of
MINERALOGY, CRYSTALLOGRAPHY, GEOCHEMISTRY, ORE DEPOSITS, PETROLOGY, VOLCANOLOGY
and applied topics on *Environment, Archaeometry* and *Cultural Heritage*

The «Flysch Rosso» shales from the southern Apennines, Italy. 1. Mineralogy and geochemistry

SAVERIO FIORE[1,*], GIUSEPPE PICCARRETA[2], FRANCESCO SANTALOIA[3], ROCCO SANTARCANGELO[1] and FRANCESCA TATEO[1]

[1] Istituto di Ricerca sulle Argille, C/da S. Loja-Area Industriale, I-85050, Tito Scalo (PZ), Italy
[2] Dipartimento Geomineralogico - Università degli Studi di Bari, Via Orabona 4, I-70124 Bari, Italy
[3] Istituto di Geologia Applicata e Geotecnica, Politecnico di Bari, Via Orabona 4, I-70124 Bari, Italy

Submitted, January 2000 - Accepted, March 2000

ABSTRACT. — A detailed mineralogical and geochemical study of the shales from the «Flysch Rosso» sediments cropping out along the front of the southern Apennines chain was conducted. Three stratigraphic sections, ranging in age from Albian to Oligocene, were investigated in order to derive information about the provenance and the depositional environment of the mudrock sediments, which show a characteristic alternation of greenish and reddish colours. Sparse rhodochrosite layers, black shales and radiolarian cherts alternations with platform-derived calcarenites and calcirudites are also present. The investigated sections include fossiliferous sediments similar to those of the Bonarelli Horizon in the Central Apennines and Southern Alps (Italy), which documents the OAE2 Cretaceous worldwide Oceanic Anoxic Event.

The mineralogy of the shales is dominated by I/S mixed layers, kaolinite, and illite; hematite is generally absent in the green shales but is ubiquitous in the reddish ones. The mineralogical composition, as well as the chemical characteristics (Al/Ti, Mg/Ni, Cr/Th, La/Sc, Th/Sc ratios and REE patterns) of the studied shales point to a Sc-poor felsic upper crust provenance.

V/Cr, Ni/Co, and U/Th ratios are indicative of overall oxic condition at the bottom-water interface. Furthermore, the absence of calcite in the shales, their very fine grain size, and the occurrence of radiolarian chert all point to a pelagic sedimentation.

RIASSUNTO. — Sono stati studiati, dal punto di vista geochimico e mineralogico, i livelli argillosi di 3 porzioni del Flysch Rosso, di età compresa tra l'Albiano e l'Oligocene, affioranti lungo il fronte dell'Appennino meridionale.

Dal punto di vista mineralogico gli shales esaminati sono composti essenzialmente da strati misti I/S, caolinite ed illite. Ematite è sempre presente nei livelli rossi ed è generalmente assente in quelli verdi.

La composizione mineralogica ed alcune caratteristiche geochimiche (come i rapporti Al/Ti, Mg/Ni, Cr/Th, La/Sc, Th/Sc, e la distribuzione delle REE) degli shales studiati indicano una provenienza da rocce della crosta superiore particolarmente povere in Sc, mentre i valori di V/Cr, Ni/Co, e U/Th suggeriscono che l'interfaccia acqua – sedimento era caratterizzata da condizioni ossidanti.

L'assenza di calcite, la granulometria estremamente fine delle particelle e la presenza di radiolariti suggeriscono un ambiente di sedimentazione di tipo pelagico.

KEY WORDS: *Shales, mineralogy, geochemistry, depositional environment, provenance, southern Apennines.*

* Corresponding author, E-mail: fiore@ira.pz.cnr.it

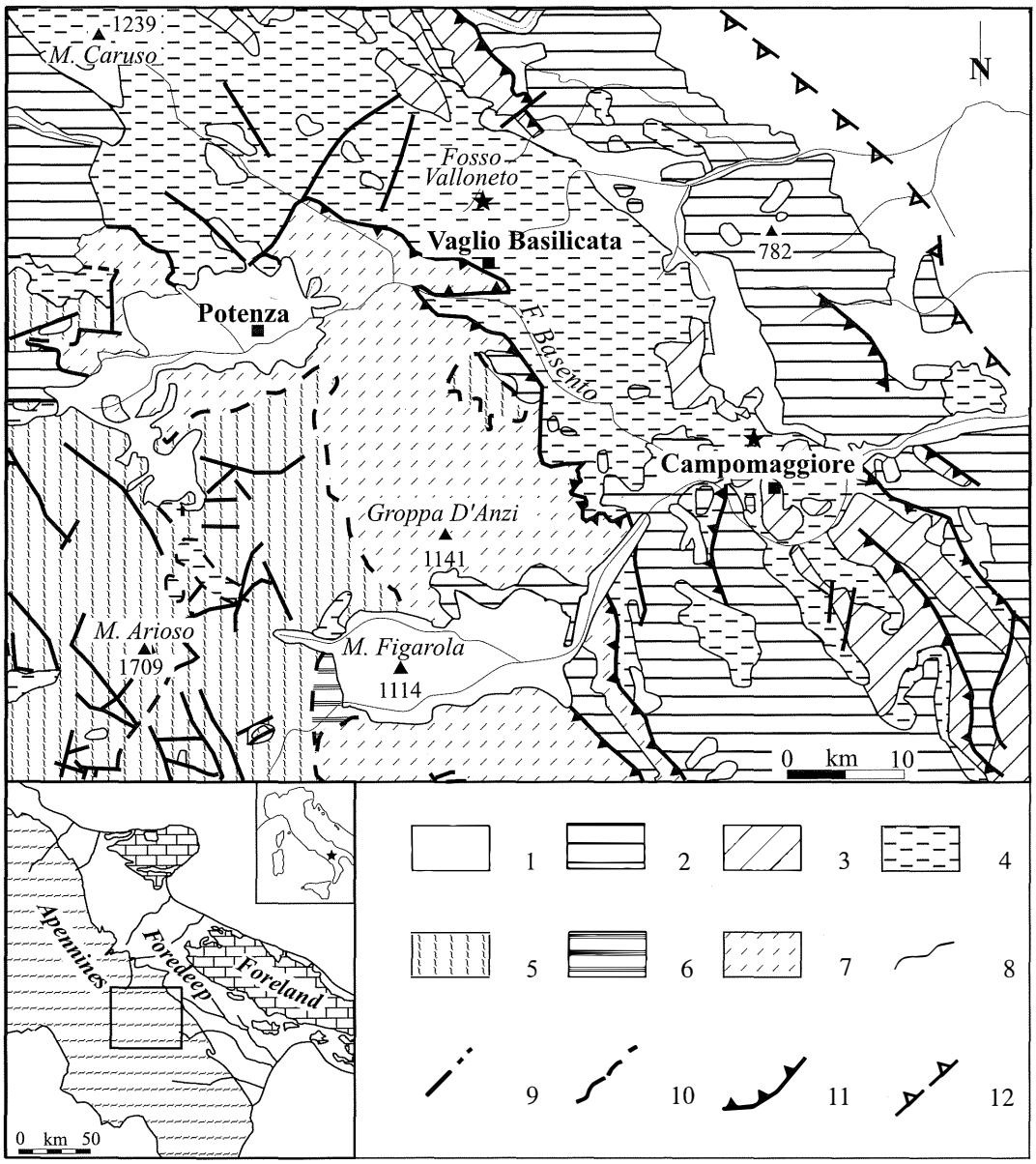

Fig. 1 – Geological sketch map of the studied area (Latitude: 40°26′23″-40°46′04″; Longitude: 15°39′17″-16°13′17″; modified after Bonardi *et al.*, 1988) and location of sample sites. 1: Holocene - Lower Pliocene; 2: Upper-Lower Miocene clastic units; 3: Numidian sandstone (Langhian-Upper Oligocene); 4: Flysch Rosso (Oligocene-Upper Cretaceous); 5: Lagonegro units (Cretaceous-Trias); 6: Nord Calabrese unit (Lower Miocene-Cretaceous); 7: Sicilide units (Lower Miocene- Cretaceous; including Argille Varicolori Formation); 8: Stratigraphic contact; 9: Faults and their inferred extension; 10: Overtrusts and their inferred extension; 11: Marginal thrusts of the Apennines chain; 12: Buried front of the Apennines chain. Star: sample site.

Introduction and Geological setting

The Apennines thrust belt formed following Tertiary eastward verging compressional events, caused by the Africa-Europe collision. It includes two major orogenic systems which coincide with the northern-central Apennines and the southern Apennines (fig. 1). In the southern Apennines thrust belt, Paleozoic crystalline units, Jurassic-Oligocene ophiolites, sedimentary units deriving from carbonate platforms, as well as from pelagic basins spanning from Lower Mesozoic to Lower Miocene were all involved.

Among the pelagic units, the «Flysch Rosso» (FR) and «Argille Varicolori» (AV) formations are widespread and the location of their palaeogeographic domain is still under debate. According to Ogniben, (1969, 1986) the two formations were deposited into two distinct pelagic basins separated by a carbonate platform. Other authors (e.g., Mostardini and Merlini, 1986; Pescatore *et al.*, 1988, 1992) attribute the AV and the FR formations to a single basin, where «Argille Varicolori» accumulated in depocentral areas.

Some contribution to elucidate depositional and post-depositional conditions, as well as the provenance of the detritus, may be obtained by mineralogical and geochemical characterization of the shales. So, we are carrying out extensive studies in order to help, through a comparative analysis, to elucidate their history, including also their pertinence to a single or to more than one basin.

In this paper we report the results of a research regarding the FR shales cropping out along the Apennines front in Basilicata to investigate on the provenance and the depositional environment.

Sampling and analytical procedures

Sampling

The samples were collected from outcrops located near Campomaggiore (Calanche and Campomaggiore successions) and Vaglio di Basilicata (Fontana Valloneto succession), along the front of the southern Apennines chain (fig. 1). The age of the studied successions ranges from Albian to Oligocene (e.g., Gallicchio *et al.*, 1996). Moreover, the radiolarian assemblages in the different successions is similar to those occurring in the Bonarelli Horizon in the Central Apennines (e.g., Marcucci Passerini *et al.*, 1991), which is related to the Cretaceous worldwide Oceanic Anoxic Events OAE2 (Schlanger and Jenkyns, 1976; Arthur *et al.*, 1990).

The Calanche succession (referred to as CM) is highly deformed and consists mainly of greenish and reddish shales interbedded with siltstone layers (from some cm up to 50 cm thick) and some thin rhodochrosite-rich beds. In the lower part of the section the greenish layers predominate whereas in the higher part the reddish ones prevail. Eighteen samples were collected, at 1-1.5 m intervals, from a well stratified 30 m – thick continuous exposure.

The Campomaggiore section (referred to as CMC), is an overturned monocline structure (Gallicchio *et al.*, 1996) lying upon the younger Numidian sandstone. It consists of greenish and reddish shale, marl, calcilutite, and calcirudite. Greenish shale predominates in the lower stratigraphic portion, where many centimetric to decimetric black shale strata are also present (Fiore and Huertas, 1995). In the upper stratigraphic portion this section includes Oligocenic sediments.

The Fontana Valloneto section (referred to as CC) has close similarities with the higher part of the CM succession. It mainly consists of reddish shale, laminated and fissile, interbedded with greenish shale. The thickness of the layers varies from some centimetres up to a few decimetres. Grey and greenish siltstone, black shale, and radiolarian chert are also present at different levels. Twelve samples were collected at 1-1.5 m intervals.

Analytical methods

Samples were disaggregated with an agate mortar, by hand, and an ultrasonic bath. The <2

μm grain-size fraction was extracted, according to Stockes' law, by settling in distilled water at 20°C.

The mineralogy of the whole rock and the clay fraction was determined by X-ray powder diffraction (XRD) analysis (Siemens D5000; Cu-Ka radiation; graphite secondary monochromator; sample spinner), according to the methods of Schultz (1964) and Shaw *et al.* (1971); reflecting factors were re-calculated for the instrumental conditions employed. Oriented samples of clay fraction were prepared by settling a suspension onto a glass slide. Air dried, glycolated (60°C overnight), and heated (200°C, 350°C, and 550°C for 2 hours) oriented slides were X-rayed for clay mineral identification. The extraction of Al-hydroxides from the intergrade region of clay minerals was accomplished according to Mirabella *et al.* (1993).

Some samples were studied by scanning electron microscopy (SEM; Cambridge S360; V = 15-25 kV; I = 100-500 pA) coupled with an energy dispersive X-ray spectrometer (EDX) and a backscattered electron detector (BSE). The finer particles were settled onto a carbon stub and the coarser particles (>32 μm, separated by wet sieving) were resin-embedded and thin sectioned.

The major and some trace elements (Ba, Rb, Sr, Y, Zr, Nb, Ni, Cr, V, and Co) of bulk rock and clay fraction were analysed by X-ray fluorescence (XRF) spectrometry on pressed powder samples. Concentrations were calculated using the matrix correction effect method (Franzini *et al.*, 1972, 1975; Leoni and Saitta, 1976). Replicate analyses of AGV-1 (USGS, USA) and NIM-G (NIM, South Africa) geostandards indicated that typical precision is better than 5% for all the elements except for Ba, for which it is better than 10%. Analyses of the rare earth elements (REE), Sc, Th, and U were carried out by inductively coupled plasma mass spectrometry (ICP-MS) at the X-Ray Assay Laboratories (Ontario, Canada). Sample dissolution was performed by fusion with Na_2O_2. Replicate analyses of solutions indicated that the precision is better than 5% except for La (<10%). FeO content was determined by titration according to Wilson's method (1960) as modified by Jeffery (1970). Loss on ignition (LOI) was measured by heating the powder in furnace at 900°C for 3 hours.

RESULTS

Mineralogy

Results of semiquantitative mineralogical whole rock analyses are summarized in Table 1. The studied shales have high contents of phyllosilicates (up to 85%), mainly dioctahedral; in the CMC section, the sum of phyllosilicates is lower than in CM and CC sections due to the higher Qtz-content. Hematite is present in all the reddish samples but in only 4 of the 24 greenish samples. SEM observations revealed the occurrence of some biotite lamellae associated with albite and the detrital morphology of clay particles. Chlorite occurs in small amounts (<4%). In the >60 μm fraction, some clinopyroxene grains have been observed.

One of the collected samples (CC 12) is a radiolarian chert composed mainly of quartz and with small amounts of calcite and dolomite. Optical observation of thin sections revealed the presence of secondary carbonates, filling the fractures, as well as the presence of remains of radiolarian shells replaced by chalcedony. Radiolarian shells were found also in shales. One of the samples collected from CM section (CM 25) is anomalous due to the presence of rhodochrosite, kutnohorite and calcite (identified by SEM-EDX). Microscopic observation evidenced the presence of rare foraminifera shells replaced by rhodochrosite.

The mineralogical composition of the <2 μm fraction is summarized in Table 1. It is characterised by high and variable quantities of an expandable phase which shows a maximum at 17 Å (glycolated sample) and a non-integral sequence of basal orders, typical of a disordered interstratified clay mineral (Moore and Reynolds, 1989). This clay phase is a

TABLE 1

Mineralogical composition (weight %) of the whole rock and of the < 2 μm fraction. Sample listed according to their stratigraphic position.

Whole rock											<2 μm fraction				
Sample	Colour	ΣPhy	Qtz	Fd	Chl	Hm	Go	Gy	Rh	Cc	Do	I-S	Ill	Ka	Chl	Qtz
CM 16	red	68	21	4	1	6						48	10	32		10
CM 17	green	79	17	3	1				tr			44	16	22		18
CM 18	green	79	19	1	1							66	13	14		7
CM 19	red	76	19	1	1	3	tr					61	12	18		9
CM 20	green	82	15	2	1							60	7	24		9
CM 21	red	78	15	2	1	4	tr					60	7	26		7
CM 22	green	78	20	1	1							72	7	12		9
CM 23	red	76	19	1	1	3	tr					64	11	19		6
CM 24	green	82	15	1	1	1						48	9	34		9
CM 25	black	39	18	1	tr	1	2	tr	32	6						
CM 26	green	76	19	2	1	1		1				58	10	25		7
CM 27	green	71	26	1	2		tr					68	7	14	tr	11
CM 28	green	81	17	1	1			tr				54	5	31		10
CM 29	red	70	20	3	tr	7	tr					55	5	34		6
CM 30	green	83	15	2	tr		tr					54	5	35		6
CM 31	red	74	20	1	2	3	tr					54	9	27		10
CM 32	green	72	26	1	1							63	7	20	tr	10
CM 33	green	82	15	2	1							55	6	22	tr	17
CMC 18	red	71	21	4	1	3						55	14	15	tr	16
CMC 16	red	53	41	2	1	3						43	12	17	tr	28
CMC 15	red	67	25	3	1	4						50	8	18	tr	24
CMC 13	red	66	25	3	2	4						56	14	13	tr	17
CMC 11	green	54	44	1	1							30	8	18	12	32
CMC 9	green	62	35	1	2							48	4	12	6	30
CMC 7	green	66	29	1	3	1						50	9	23	tr	18
CMC 5	green	55	41	1	3							29	16	12	12	32
CMC 3	green	63	31	2	4							48	7	16	5	24
CMC 1	green	64	30	3	3							51	7	14	6	22
CC 25	red	76	17	2	2	3						56	7	23	3	11
CC 24	red	77	20	1	1	1						37	14	25	3	21
CC 23	green	69	30		1							36	17	11	3	33
CC 22	green	74	25	1	1							63	8	11	2	16
CC 21	green	72	27	1	1							61	10	8	2	19
CC 20	green	76	20	2	1	1						55	10	14	4	19
CC 19	red	75	18	2	1	4						58	10	16	3	13
CC 18	green	79	15	4	1							51	26	10	3	10
CC 17	green	83	14	2	1							64	13	13	3	7
CC 16	green	72	25	3	1							73	5	6	3	13
CC 15	red	74	18	4		3						68	11	6	2	13
CC 12	grey		92		4					2	2					
CC 11	green	69	23	4		5						69	15	1	1	14

ΣPhy = phyllosilicate (chlorite excluded); Qtz = quartz; Fd = feldspars; Chl = chlorite; Hm = hematite; Go = goethite; Gy = gypsum; Rh = rhodochrosite; Cc = calcite; Do = dolomite; I-S = interstratified illite-smectite; Ill = illite; Ka = kaolinite. CM = Calanche section; CMC = Campomaggiore section; CC = Fontana Valloneto section.

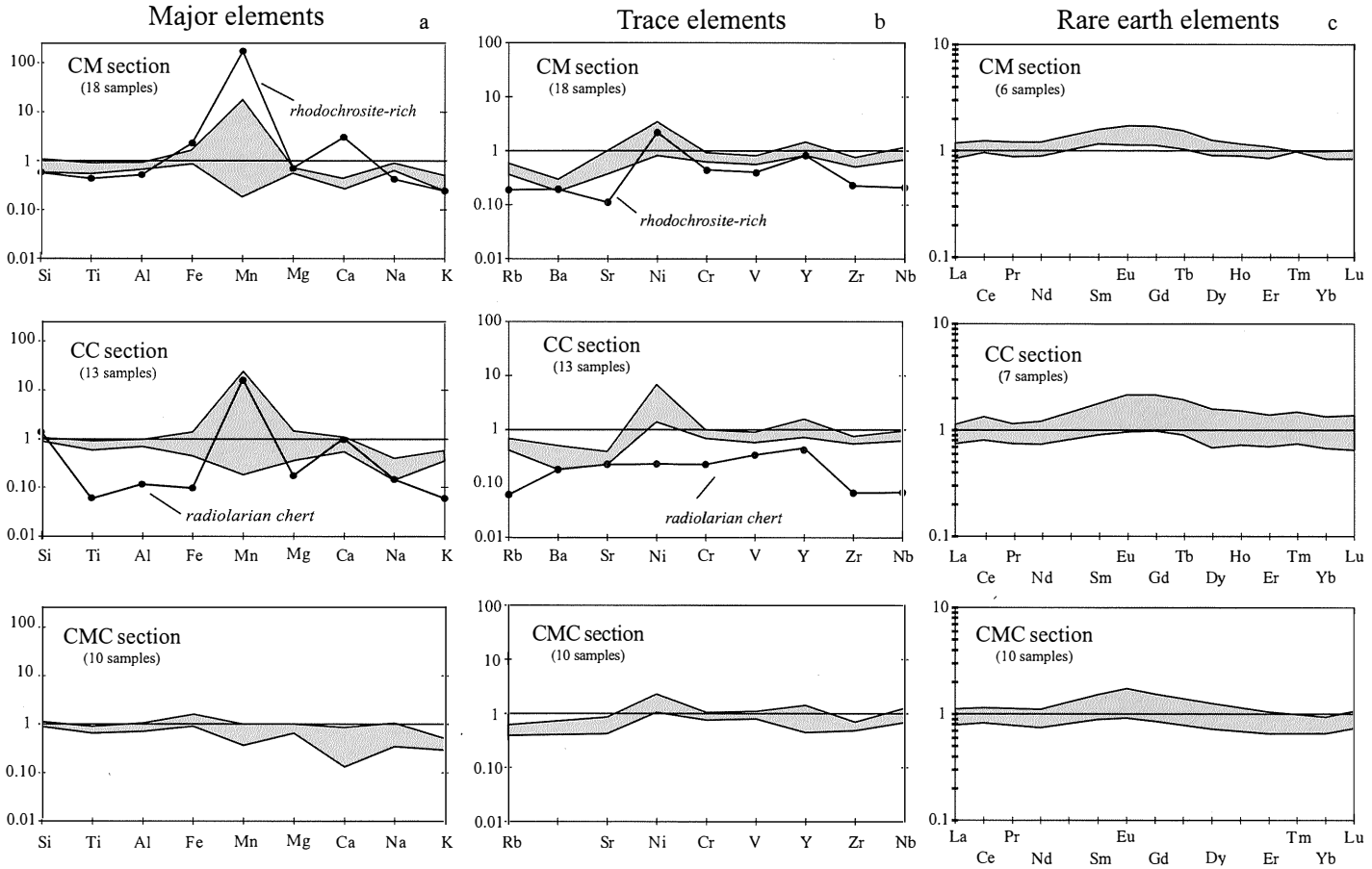

Fig. 2 – Major and trace element compositional ranges of the «Flysch Rosso» shales. The values are normalized to PAAS (McLennan, 1989).

random I/S mixed-layer with low illite content (I/S = 10-40). The I/S phase from CC samples differ from that of the others because of the presence of Al-hydroxides in the intergrade region. In addition, it appears that the I/S mixed-layer within the shales of the CM and CMC sections is distinct from that of the CC section, which is Ca-richer (see later). Illite, here referred to as a 10 Å mineral(s) unaffected by ethylene-glycol treatment, shows a large range of content (Table 1). Also the amount of kaolinite is variable and more abundant in samples from CM section. The I/S mixed-layer decidedly prevails in all the samples and its content appears antipathetically correlated with kaolinite or quartz contents which are generally higher in CM and CMC sections, respectively (Table 1). Finally, chlorite is scarce or at trace level but some samples of the CMC section. Illite in the CM and CMC sections tends to increase upward and chlorite tends to be more abundant in the lower levels of the CMC section.

Geochemistry

Elemental abundance and some elemental ratios are reported in Table 2 and illustrated in fig. 2 as normalised to Post-Archean Average Australian Shale (PAAS; McLennan, 1989).

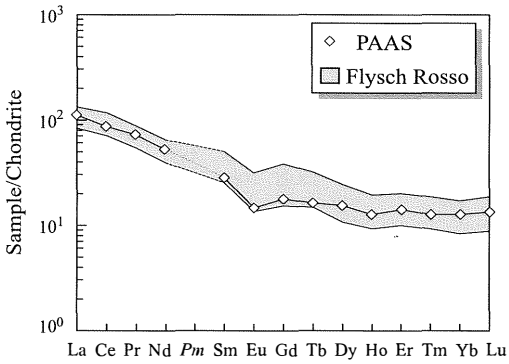

Fig. 3 – Compositional range of chondrite-normalized REE (Wakita *et al.*, 1971) distribution in the «Flysch Rosso» shales. An estimate of upper crustal abundances (PAAS; Taylor and McLennan, 1985) is plotted for reference.

REE contents are also given as normalized to chondrite values (Wakita *et al.*, 1971) in fig. 3. The most evident feature is the very high spread of Mn-content in the samples of CC and CM sections. The high enrichment in some samples does not coincide with the presence of rhodochrosite. As a matter of fact, the Mn-content of the radiolarian chert (sample CC12), for example, is about 16 times the PAAS and is due to the presence of poorly crystalline and amorphous Mn-hydroxides occurring as metallic lustre film coating fissured blocks. The other elements except Fe are depleted relative to PAAS; in particular K in the three sets, Na in CC samples, and Ca in samples from CM and CMC sections.

The radiolarian-rich sample (CC 12), besides the obvious Si enrichment, shows an appreciable amount of Al, which is in contrast with the scarceness of phyllosilicates; aluminium may be related, however, to biogenic processes as will be discussed in the following.

Reddish and greenish shales have overall similar major-element compositions (Table 2) even if they exhibit some differences. The red shales have higher Fe_2O_3 and lower SiO_2 and FeO contents, as well as lower values of Al/Ti and $Fe^{2+}/(Fe^{2+}+ Fe^{3+})$ ratios. The lower SiO_2 content in the red shales is a consequence of the higher iron content which dilutes the other oxides. A positive linear correlation exists between the phyllosilicates and their iron content (roughly calculated by subtracting Fe_2O_3 in hematite from the total Fe_2O_3 content), but there is a lower statistical significance between Al_2O_3 and $Fe_2O_{3(Phy)}$ and between Al_2O_3 and ΣPhy (fig. 4): this also suggests the presence of amorphous Al-rich component in the studied shales. Aluminium may be involved in the biogenic processes (e.g., van Bennekom *et al.*, 1989) and/or scavenged from seawater (e.g., Murray and Leinen, 1996) and therefore it cannot be simply related to clay minerals. The FeO content is unrelated to the I/S and kaolinite abundance and it is negatively correlated to illite. Finally, no relationship exists between $Fe_2O_{3(Phy)}$ and

TABLE 2

Chemical composition and some elemental ratios of the whole rock of the «Flysch Rosso» shales. Major elements as percent oxides and trace elements in ppm. Samples from the top to the bottom in the sections are arranged from left to right in the table.

Sample	CM16	CM17	CM18	CM19	CM20	CM21	CM22	CM23	CM24	CM25	CM26	CM27	CM28	CM29	CM30	CM31
Colour	red	green	green	red	green	red	green	red	green	black	green	green	green	red	green	red
SiO_2 (wt%)	60.09	62.26	63.44	58.93	62.34	60.07	63.92	57.91	60.65	35.90	58.47	67.65	67.94	58.05	62.53	57.30
TiO_2	0.77	0.73	0.69	0.79	0.79	0.82	0.68	0.77	0.91	0.43	0.80	0.56	0.68	0.85	0.79	0.77
Al_2O_3	15.75	15.63	14.40	16.57	16.36	17.44	14.73	15.95	17.94	9.69	17.82	12.69	15.16	17.72	17.47	16.48
Fe_2O_3*	10.37	5.34	6.03	8.72	7.48	9.49	6.34	9.78	7.19	14.68	6.51	6.54	5.69	10.56	6.62	10.09
MnO	0.02	1.95	0.77	0.04	0.10	0.03	0.02	0.06	0.05	19.00	0.25	0.02	0.07	0.03	0.03	0.05
MgO	1.45	1.61	1.57	1.44	1.58	1.42	1.42	1.48	1.43	1.57	1.47	1.53	1.23	1.33	1.36	1.37
CaO	0.54	0.47	0.54	0.42	0.45	0.42	0.41	0.43	0.53	3.97	0.57	0.37	0.41	0.50	0.43	0.47
Na_2O	0.96	1.01	1.01	0.98	1.08	1.09	0.93	1.07	1.03	0.51	1.01	0.77	0.84	0.93	0.91	0.98
K_2O	1.55	1.86	1.38	1.49	1.41	1.38	1.16	1.44	1.45	0.89	1.40	1.03	0.92	1.21	1.09	1.44
P_2O_5	0.12	0.07	0.05	0.07	0.08	0.07	0.07	0.08	0.13	0.16	0.10	0.08	0.06	0.08	0.08	0.10
LOI	8.44	9.07	10.14	10.59	8.41	7.81	10.40	11.10	8.74	13.18	11.74	8.95	7.10	8.75	8.86	11.75
Corg	0.06	0.29	0.09	0.07	0.07		0.06	0.06	0.10		0.09	0.08	0.12	0.09	0.09	0.06
Ba (ppm)	153	167	151	152	181	153	147	141	192	126	172	119	138	174	194	160
Ni	73	88	80	69	79	66	68	57	79	121	190	50	59	76	73	54
Cr	90	87	80	94	90	101	81	92	99	49	93	71	82	103	95	93
V	102	121	101	102	99	112	105	110	127	60	121	99	102	123	123	100
Rb	93	94	79	91	88	86	74	90	91	30	86	64	58	77	70	89
Sr	107	108	100	93	107	105	99	104	123	22	104	84	97	116	106	105
Y	37	24	22	24	30	24	25	28	39	22	28	23	22	25	26	31
Zr	134	133	125	137	137	134	122	135	159	47	142	112	122	144	142	135
Nb	17	14	14	16	17	18	14	17	22	4	18	13	16	20	19	17
Sc			5.5	5.6				5.5			5.9					6.1
Co			29	20				18			85					11
Th			9.6	10.7				10.6			11.6					10.9
U			2.5	1.5				1.4			1.6					1.2
La			34.8	38.5				40.7			45.7					45
Ce			76.6	83.0				87.0			98.8					93.2
Pr			7.8	8.6				9.4			10.5					10.7
Nd			30.1	33.4				34.8			41.2					40.2
Sm			6.4	6.8				8.1			8.8					8.8
Eu			1.24	1.44				1.68			1.8					1.88
Gd			5.3	6.1				5.8			7.6					7.8
Tb			0.8	1				1			1.2					1.2
Dy			4.2	4.4				5			5.6					5.9
Ho			0.88	0.92				1.16			1.12					1.16
Er			2.4	2.4				2.8			2.9					3.10
Tm			0.4	0.4				0.4			0.4					0.4
Yb			2.4	2.5				2.5			2.5					2.8
Lu			0.36	0.36				0.36			0.4					0.44
ΣREE			173.68	189.82				201.7			228.52					222.58
CIW	87	87	85	88	87	88	88	87	88	56	88	88	88	89	89	88
Fe_2O_3	9.81		5.92	8.50	6.70	9.16	5.45	9.22	6.63		5.18	4.65	4.69	10.00	4.95	9.31
FeO	0.50		0.10	0.20	0.70	0.30	0.80	0.50	0.50		1.20	1.70	0.90	0.50	1.50	0.70
$Fe_2O_{3(Phy)}$	3.81		5.92	5.50	6.70	5.16	5.45	6.22	5.63		4.18	4.65	4.69	3.00	4.95	6.31
$Fe^{2+}/(Fe^{2+}+Fe^{3+})$	0.05		0.02	0.03	0.10	0.04	0.14	0.06	0.08		0.20	0.29	0.18	0.05	0.25	0.08
U/Th			0.26	0.14				0.13			0.14					0.11
V/Cr	1.13	1.39	1.26	1.09	1.10	1.11	1.30	1.19	1.28	1.22	1.31	1.38	1.24	1.19	1.29	1.08
Al/Ti	18.07	18.91	18.43	18.53	18.29	18.78	19.13	18.30	17.41	19.90	19.67	20.01	19.69	18.41	19.53	18.90
Ni/Co			2.76	3.45				3.17			2.24					4.89
Th/Sc			1.75	1.91				1.93			1.97					1.79
La/Sc			6.33	6.88				7.40			7.75					7.38
Cr/Th			10.10	9.27				8.36			7.75					8.64
Eu/Eu*			0.66	0.69				0.70			0.68					0.70

Fe_2O_3*: including FeO as Fe_2O_3. $Fe^{2+}/(Fe^{2+}+Fe^{3+})$ as molar ratio. Europium anomaly (Eu/Eu*) is calculated using the ratio between Eu normalized to chondrite value (Eu_{sample}/Eu_{ch}) and Eu*, where Eu* is $[(Sm_{sample}/Sm_{ch}) \times (Gd_{sample}/Gd_{ch})]^{0.5}$. Chondrite values from Wakita *et al.* (1971).

TABLE 2, *continued*

Sample	CM32	CM33	CMC18	CMC16	CMC15	CMC13	CMC11	CMC9	CMC7	CMC5	CMC3	CMC1
Colour	green	green	red	red	red	red	green	green	green	green	green	green
SiO_2 (wt%)	67.77	65.37	57.38	68.54	62.61	59.23	69.99	65.83	60.40	68.17	61.73	63.14
TiO_2	0.55	0.64	0.86	0.69	0.83	0.90	0.69	0.70	0.88	0.66	0.81	0.73
Al_2O_3	12.66	14.80	18.99	13.72	16.65	18.71	14.88	16.63	20.08	14.83	17.82	18.15
Fe_2O_3*	6.36	6.78	9.00	7.99	9.50	9.98	5.71	6.48	6.84	7.17	8.88	6.60
MnO	0.03	0.03	0.11	0.04	0.06	0.05	0.04	0.07	0.05	0.05	0.04	0.05
MgO	1.41	1.43	2.21	1.47	1.49	1.52	1.44	1.68	1.57	1.57	1.68	1.86
CaO	0.44	0.41	1.13	0.36	0.28	0.31	0.24	0.37	0.27	0.20	0.17	0.31
Na_2O	0.99	1.00	0.41	1.02	1.15	1.26	0.84	0.59	0.97	0.92	1.16	0.71
K_2O	0.99	0.95	1.92	1.51	1.34	1.70	1.09	1.12	1.48	1.20	1.53	1.31
P_2O_5	0.11	0.05	0.06	0.08	0.06	0.11	0.05	0.06	0.07	0.07	0.05	0.05
LOI	8.86	8.71	6.90	5.41	5.99	5.67	6.25	7.03	6.94	6.04	5.94	7.14
Corg	0.08	0.11										
Ba (ppm)	118	124	178	190	240	185	325	204	165	175	178	126
Ni	45	70	127	74	91	64	64	72	64	58	113	59
Cr	69	76	115	88	103	111	83	92	113	90	109	106
V	83	112	166	118	127	135	124	152	162	124	131	129
Rb	63	62	98	85	81	96	67	62	85	74	93	79
Sr	75	92	173	98	112	129	94	87	112	84	126	89
Y	31	20	22	23	21	38	19	22	28	15	12	22
Zr	106	113	128	128	130	148	134	116	140	102	136	120
Nb	13	16	21	13	16	24	15	22	24	14	21	23
Sc	5.5											
Co	15											
Th	8.6											
U	1.2											
La	32.2		36	32.7	34.6	42.2	30.8	33.9	42.9	30.3	33.1	31.2
Ce	88.2		75.2	66.7	73.5	85.2	65.5	74.1	91.6	74.6	71.3	70.1
Pr	8.6											
Nd	34.1		30.4	29.7	29.8	37.7	26.4	28.7	36.4	27.9	28.4	25.3
Sm	8.7		6.1	6.3	6.1	8.5	5	5.8	7.1	5.8	5.6	5.1
Eu	1.88		1.35	1.36	1.31	1.87	1.05	1.19	1.58	1.27	1.16	0.99
Gd	8		5.11	5.16	4.85	7.23	4	4.73	5.38	4.96	4.27	4.21
Tb	1.2											
Dy	5.4		4.3	4.28	4.23	5.86	3.52	3.88	4.69	4.04	4	3.38
Ho	1.08											
Er	2.7		2.52	2.82	2.25	3	1.86	2.18	2.47	2.48	2.35	2.05
Tm	0.4											
Yb	2.4		2.23	2.14	2.12	2.65	1.84	1.94	2.34	2.1	2.19	1.84
Lu	0.36		0.37	0.36	0.36	0.46	0.32	0.34	0.37	0.37	0.39	0.35
ΣREE	195.22		163.59	151.35	159.15	194.58	140.34	156.75	194.84	153.77	152.55	144.41
CIW	85	87	88	87	88	89	90	92	91	90	90	92
Fe_2O_3	4.69	5.11	7.98	6.50	8.17	8.55	2.98	3.49	4.41	3.44	5.58	3.43
FeO	1.50	1.50										
$Fe_2O_{3\,(Phy)}$	4.69	5.11	4.98	3.50	4.17	4.55	2.98	3.49	3.41	3.44	5.58	3.43
$Fe^{2+}/(Fe^{2+}+Fe^{3+})$	0.26	0.25										
U/Th	0.14											
V/Cr	1.21	1.47	1.44	1.34	1.23	1.22	1.49	1.65	1.43	1.38	1.20	1.22
Al/Ti	20.33	20.42	19.50	17.56	17.72	18.36	19.05	20.98	20.15	19.85	19.43	21.96
Ni/Co	3.02											
Th/Sc	1.56											
La/Sc	5.85											
Cr/Th	7.76											
Eu/Eu*	0.70		0.74	0.74	0.75	0.74	0.73	0.70	0.79	0.73	0.73	0.66

Fe_2O_3*: including FeO as Fe_2O_3. $Fe^{2+}/(Fe^{2+}+Fe^{3+})$ as molar ratio. Europium anomaly (Eu/Eu*) is calculated using the ratio between Eu normalized to chondrite value (Eu_{sample}/Eu_{ch}) and Eu*, where Eu* is $[(Sm_{sample}/Sm_{ch}) \times (Gd_{sample}/Gd_{ch})]^{0.5}$. Chondrite values from Wakita *et al.* (1971).

TABLE 2, *continued*

Sample	CC25	CC24	CC23	CC22	CC21	CC20	CC19	CC18	CC17	CC16	CC15	CC12	CC11
Colour	red	red	green	green	green	green	red	green	green	green	red	grey	red
SiO_2 (wt%)	55.34	61.14	67.94	67.18	68.92	63.38	59.52	57.62	58.55	64.96	59.83	90.26	60.05
TiO_2	0.87	0.73	0.58	0.70	0.65	0.75	0.81	0.83	0.89	0.73	0.77	0.06	0.65
Al_2O_3	18.15	16.11	13.13	15.32	13.56	14.82	16.16	16.95	17.91	13.88	14.75	2.26	14.77
Fe_2O_3*	8.67	7.76	5.63	2.78	4.12	7.58	8.35	8.24	5.79	4.57	8.18	0.63	7.29
MnO	0.30	0.05	0.11	0.02	0.09	0.03	0.04	0.08	0.04	0.94	0.04	1.83	0.05
MgO	1.32	1.10	1.47	1.21	1.24	1.52	1.77	2.15	2.20	1.82	2.18	0.39	3.16
CaO	0.90	0.80	0.70	0.74	0.72	0.81	0.91	1.12	0.88	0.91	1.14	1.34	1.41
Na_2O	0.24	0.17	0.23	0.28	0.25	0.28	0.24	0.35	0.35	0.35	0.35	0.18	0.47
K_2O	1.37	1.28	1.41	1.33	1.33	1.64	1.53	2.04	1.95	1.30	1.67	0.23	2.07
P_2O_5	0.07	0.09	0.05	0.05	0.05	0.12	0.09	0.07	0.07	0.09	0.11	0.16	0.28
LOI	12.77	10.80	8.82	10.42	9.10	9.23	10.65	10.61	11.55	10.45	11.05	2.66	9.84
Corg		0.04	0.04		0.10	0.04	0.03	0.03			0.03		0.01
Ba (ppm)	324	136	205	142	194	127	114	129	126	135	141	117	132
Ni	88	77	115	103	84	65	84	282	377	320	109	13	77
Cr	103	86	76	92	85	88	97	107	111	85	97	25	76
V	117	95	105	137	121	92	105	121	133	109	98	51	86
Rb	86	80	81	77	76	92	85	105	100	66	90	10	108
Sr	78	68	59	68	68	76	70	63	64	76	71	45	50
Y	26	30	19	22	21	43	31	27	28	28	35	12	38
Zr	147	124	115	143	132	145	142	144	160	131	149	14	122
Nb	18	15	12	15	14	16	16	16	18	15	17	1	14
Sc	5.7		5.6	5.9	5.0	5.0			6.4				6.0
Co	28		53	35	65	15			146				23
Th	10.6		8.2	10.1	9.1	9.7			10.1				11.4
U	1.2		3.8	7.1	4.0	1.1			5.7				1.2
La	40.9		28.4	33.6	32.7	41.1			38.9				43.5
Ce	83.6		64.3	73.1	68.3	90.9			88.6				107
Pr	9.2		6.6	8.3	8	10.2			9.2				10.1
Nd	35.7		24.9	31.3	31	41			33.5				39.4
Sm	8.1		5	6.0	6.2	9.9			7.4				9
Eu	1.76		1.04	1.2	1.28	2.32			1.6				2
Gd	7.1		4.60	5.6	5.2	10.1			6.4				9.8
Tb	1		0.7	0.8	0.8	1.5			0.8				1.4
Dy	4.8		3.2	4.3	3.8	7.4			5				7.2
Ho	0.96		0.72	0.88	0.8	1.52			1.04				1.52
Er	2.4		2	2.4	2.3	3.8			2.6				4
Tm	0.4		0.3	0.3	0.4	0.5			0.4				0.6
Yb	2.4		1.9	2.4	2.6	3.4			2.6				3.8
Lu	0.36		0.28	0.36	0.36	0.48			0.4				0.6
ΣREE	198.68		143.94	170.54	163.74	224.12			198.44				239.92
CIW	91	91	90	90	89	90	90	87	90	87	86	49	85
Fe_2O_3		7.43	4.93	2.34	3.79	6.20	7.65	7.59	4.01		7.58		7.01
FeO		0.30	0.63	0.40	0.30	1.24	0.63	0.59	1.60		0.54		0.25
$Fe_2O_{3\,(Phy)}$		6.43	4.93	2.34	3.79	5.20	3.65	7.59	4.01		4.58		2.01
$Fe^{2+}/(Fe^{2+}+Fe^{3+})$		0.04	0.12	0.16	0.08	0.18	0.08	0.08	0.31		0.07		0.04
U/Th	0.11		0.46	0.70	0.44	0.11			0.56				0.11
V/Cr	1.14	1.11	1.38	1.48	1.43	1.05	1.08	1.13	1.20	1.29	1.01	2.07	1.13
Al/Ti	18.43	19.49	19.99	19.33	18.43	17.45	17.62	18.04	17.77	16.79	16.92	33.27	20.07
Ni/Co													
Th/Sc	1.86		1.46	1.71	1.82	1.94			1.58				1.90
La/Sc	7.18		5.07	5.69	6.54	8.22			6.08				7.25
Cr/Th	9.36		9.50	9.20	9.44	8.80			11.10				6.91
Eu/Eu*	0.72		0.67	0.64	0.70	0.72			0.72				0.66

Fe_2O_3*: including FeO as Fe_2O_3. $Fe^{2+}/(Fe^{2+}+Fe^{3+})$ as molar ratio. Europium anomaly (Eu/Eu*) is calculated using the ratio between Eu normalized to chondrite value (Eu_{sample}/Eu_{ch}) and Eu*, where Eu* is $[(Sm_{sample}/Sm_{ch}) \times (Gd_{sample}/Gd_{ch})]^{0.5}$. Chondrite values from Wakita *et al.* (1971).

the single clay mineral, but a multiple correlation is statistically significant ($p = 0.02$) and this indicates that they, all together, exert a control on the iron abundance.

The chemical index of weathering (CIW; Harnois, 1988) varies within a narrow range (85-91; Table 2) and this could be interpreted as indicative of intense weathering of the source(s) area(s) and absence of important climatic changes over time. However, some peculiarites emerge when plotting CIW-values versus CaO and Na_2O contents (fig. 5*a-b*). The samples from section CC portray a distinct trend being richer in CaO and poorer in Na_2O. This might indicate that the I/S mixed-layers occurring in the shales from the CM and CMC sections are distinct from those occurring in the CC section. To clarify this aspect, a leaching test on clay fraction carried out by ammonium acetate, a reactant able to remove specific and non specific adsorbed cations, evidenced that Na and Ca are in interlayer positions or adsorbed onto clay particles. The presence of these cations in exchangeable positions suggests some caution in interpreting CIW index of shales as indicative of the intensity of weathering of the sources. Shales might represent, for example, recycled older fine sediments and in this case chemical indices of alterations monitor their characteristics and not intensity of weathering.

As concerns the trace elements, the abundance of Rb, Ba, Sr, Ni, Cr, V, Y, Zr, and Nb are plotted in fig. 2*b* as normalized to PAAS.

Ni concentrations are comparable to PAAS except for five samples from CC section in which it is strongly enriched (up to 377 ppm) determining a positive spike in figure 2*b*; Y and Nb are slightly enriched or depleted. The other trace elements are more or less depleted, especially Ba, Rb and Sr, most likely reflecting the low feldspar content of the «Flysch Rosso» shales.

Sc, Co, Th, and U were not plotted in the spiderdiagram because they were not determined in all the samples. Sc, Th and U are decidedly lower than in PAAS and vary within

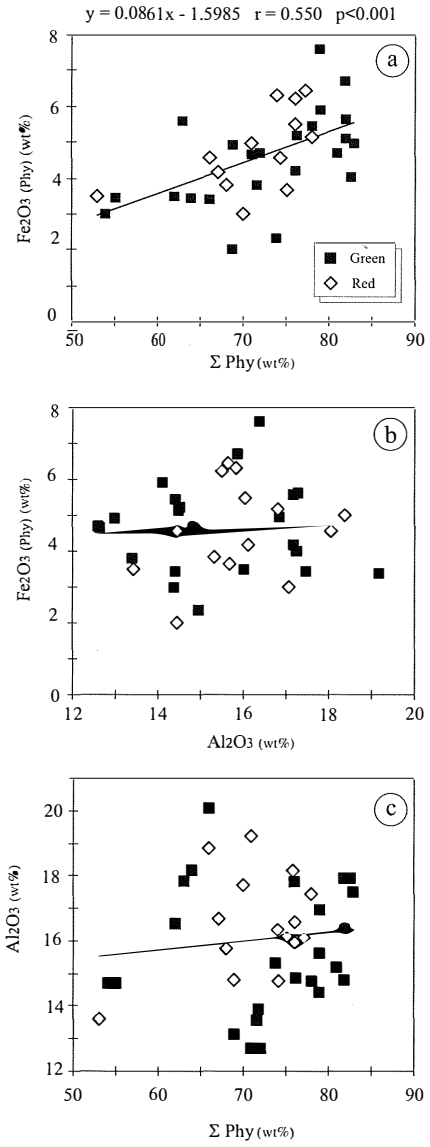

Fig. 4 – (*a*) Fe_2O_3 content of phyllosilicates ($Fe_2O_{3(Phy)}$), calculated subtracting Fe_2O_3 of the hematite, vs. the amount of phyllosilicates (ΣPhy) for the «Flysch Rosso» shales. (*b*) $Fe_2O_{3(Phy)}$ vs. Al_2O_3 content of the shales from the «Flysh Rosso» shales. (*c*) Al_2O_3 vs. ΣPhy for the «Flysch Rosso» shales. The statistical linear correlation in (*a*) indicates the control of clay minerals on the abundance of Fe_2O_3 (see text). The absence of correlation between Al_2O_3 - ΣPhy and Al_2O_3-$Fe_2O_{3(Phy)}$ (*b, c*) suggests that Al is not exclusively related to clay minerals and that other Al-carriers are present.

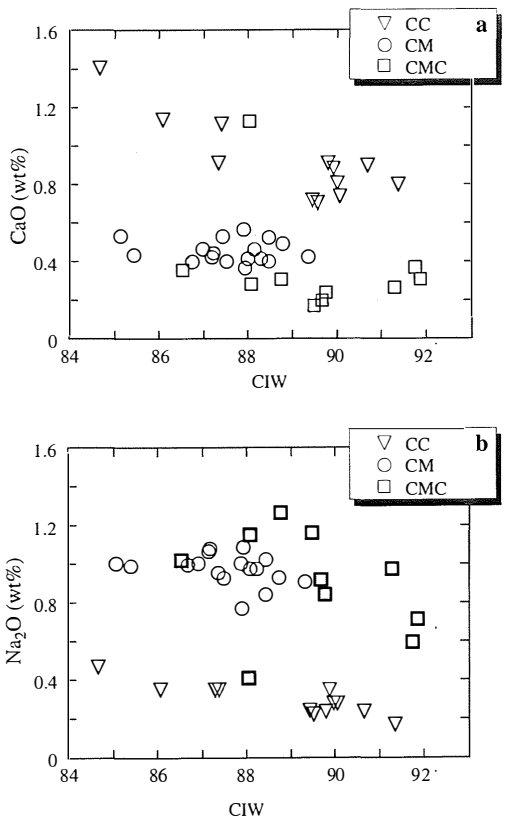

Fig. 5 – Plots of Chemical Index of Weathering (CIW, Harnois, 1988) vs. CaO (*a*) and Na_2O (*b*) abundance for the «Flysch Rosso» shales. Samples from Campomaggiore and Calanche successions have lower CaO and higher Na_2O than the samples from Fontana Valloneto succession, most likely as a consequence of the presence of a distinct type of smectite (see text). CIW = $[Al_2O_3/(Al_2O_3 + CaO + Na_2O)] \times 100$ in molecular proportions. CaO is that in silicates and it is calculated by subtraction of apatite assuming all P_2O_5 forming apatite.

a narrow range; Co values instead are scattered (11-146 ppm). A strong statistical relationship exists between Ni and Co (fig. 6) and Ni/Co ratio has mostly an average of 2.2. The Cr/Th and Sc/Th ratios concentrate between 8-10 and 0.5-0.6, respectively.

Thirteen samples representative of reddish and greenish shales were analysed for REE content (Table 2). ΣREE vary from ≈140 ppm up to ~240 ppm and the chondrite-normalised patterns are quite similar to post-Archean shales (fig. 3), with LREE enrichment, an almost flat HREE pattern, and a negative Eu-anomaly with Eu/Eu* ranging from 0.64 to 0.79 ($x = 0.71 \pm 0.01$). The MREE contents are enriched with respect to PAAS (fig. 2*c*). V content is higher and Cr is lower in the green shales, and therefore the V/Cr ratio in the two chromatic types has a high statistical significance ($p = 0.0013$).

DISCUSSION AND CONCLUSIONS

The «Flysch Rosso» successions here studied show few mineralogical differences. The Campomaggiore sections include shales which are richer in quartz and chlorite relatively to the CM and CC shales. The chlorite content is higher in the lower part of CMC section whereas illite content tends to be higher towards the top of CM section.

In spite of the above differences, the shales collected from distinct outcrops are quite similar thus suggesting that changes related to space and/or time seem to be negligible. Nevertheless, the higher quartz and chlorite contents in the CMC section, which includes also more recent terrains with respect to the other ones, might reflect some changes in time.

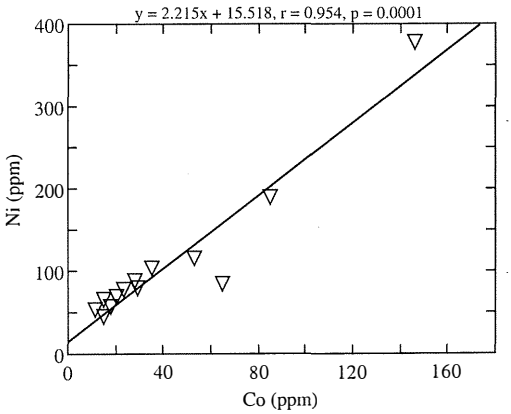

Fig. 6 – Plot of Ni vs. Co for the «Flysch Rosso» shales. Although the elemental concentrations vary widely, Ni/Co has a constant average value (~ 2.2).

The scarcity of chlorite is indicative of the felsic nature of the source. Also some geochemical indices are indicative of the felsic nature of the source of the shales and of its overall homogeneity. MgO-Cr and MgO-Ni relationships have been modelled by Van de Kamp and Leake (1985) to define contribution from felsic and mafic-ultramafic end members.The shales here studied display MgO-Ni-Cr (not reported) relationships which are indicative of felsic provenance. Also the abundance of La, Th, Cr and Sc and their reciprocal relationships discriminate silicic and basic provenance of fine sediments (e.g., Wronkiewicz and Condie, 1989, 1990; Condie and Wronkiewicz, 1990; Cullers, 1994a, b). Cr might be a mobile element if oxidized to Cr^{6+} (Middelburg *et al.*, 1988). Mongelli *et al.* (1996) suggested that fractionation of Cr/Th ratio during weathering may cause a negative correlation between Cr/Th and Sc/Th. In our samples these ratios are statistically unrelated and therefore the Cr/Th may be considered in this case as a reliable indicator of provenance. The high La/Sc and Th/Sc and the low Cr/Th values are all indicative of a felsic continental source and this is in agreement with the REE pattern of the shales paralleling modelled by Taylor and McLennan (1985) for the upper continental crust (fig. 3). The Sc content in our shales is two to three times lower than those regarding shales of the various ages as reported by Taylor and McLennan (1985) indicating a generally poor Sc component in the source areas.

An intense chemical weathering in the source areas might be suggested by the the fact that I/S phase has high smectite contents and that the CIW values (88±2) are high. However, recycling of older sediments is possible too.

Continental and oceanic contribution might be also discriminated by the Al/Ti ratio (Boström *et al.*, 1969). However, this should be used with care because *i)* the content of Al might be modified by biogenic processes since it is involved in the construction and dissolution of siliceous organisms (e.g., van Bennekom *et al.*, 1989) and/or scavenged from sea water (e.g., Murray and Leinen, 1996); *ii)* the Ti content might depend on grain size of the sediment (e.g., Pearce and Jarvis, 1992; Calvert *et al.*, 1996). Therefore, the role of Al and Ti in marine sediments should be considered on a case-by-case basis and assessed by analyses of other geochemical indicators (Murray and Leinen, 1996). In the present study, *i)* the terrigenous component is decidedly dominant with respect to the biogenic one, except for the radiolarian chert (CC 12) and *ii)* the grain size of the shales is comparable with the database of Boström *et al.* (1969). The Al/Ti ratio ranges from 17 to 22 and this is in accordance with the other geochemical indices which suggest a continental source.

A relevant mineralogical feature is the absence of calcite, except for two samples, clearly indicating that the studied sediments accumulated beneath the carbonate compensation depth (CCD). The small grain size of terrigenous particles and the occurrence of red clays suggest deep marine sedimentation (e.g., Pickering *et al.*, 1989; Seibold and Berger, 1996) in agreement with the general interpretation of Cretaceous varicoloured clays (e.g., Eicher and Diner, 1991).

Some selected elemental ratios are currently used as monitors of palaeoenvironment conditions (e.g., Dypvik, 1984; Dill, 1986; Jones and Manning, 1994). Among the geochemical indices reflecting the redox condition in fine grained sediment, V/Cr and U/Th ratios have been proposed as the most reliable (Jones and Manning, 1994). The values calculated for the studied shales vary within a narrow range and are characteristic of overall oxic conditions (fig. 7), both for the greenish and the reddish samples even though the red shales monitor an oxygen richer environment. Also the Ni/Co ratio has been considered as a redox index (e.g., Dypvik, 1984; Dill, 1986; Jones and Manning, 1994). In the studied case the quasi constant Ni/Co ratio (fig. 6) indicative of their coherent behaviour also points to oxic conditions and this is also reinforced by the absence of appreciable amounts of sulphides in the shales. The

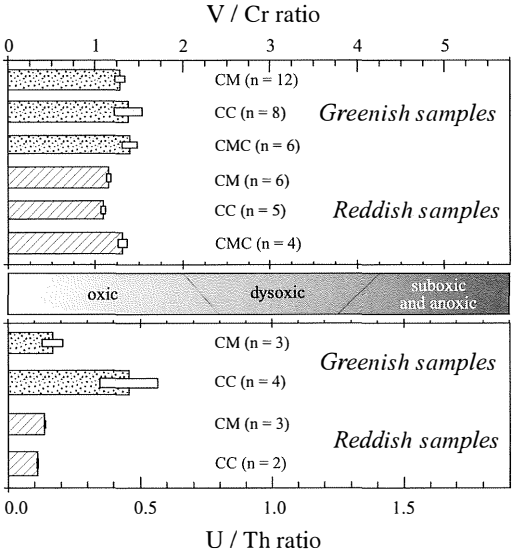

Fig. 7 – V/Cr and U/Th ratios of the samples of the «Flysch Rosso». The ratios are considered as indicative of bottom water paleo-oxygen concentration (Jones and Manning, 1994). Bars indicate the standard deviation.

possibility that the shales were rapidly deposited, bringing with them and maintaining a signature derived from an oxidised source area, must be discounted since the sedimentation rate in the «Flysch Rosso» basin was actually very low (e.g., Scandone, 1972). However, the chemical conditions at the sea-bottom experienced episodic and dramatic variations from oxic conditions to anoxic ones, as documented by the presence of the black shale layers containing up to 10% of organic carbon.

Summing up, mineralogical and geochemical data relative to Albian-Oligocenic reddish and greenish shales from the «Flysch Rosso» cropping out along the front of the Lucanian Apennines display overall homogeneity, apart from some minor differences in space and time. The shales, accumulated in a pelagic environment below the CCD, were mainly supplied from felsic continental area(s) decidedly poor in Sc. Geochemical indicators of bottom water paleo-oxygen concentration, indicate overall oxic conditions with episodic changes related to the deposition and evolution of organic rich black shales.

ACKNOWLEDGMENTS

Financial support for this study was provided by CNR. SEM observations and XRF analyses were performed at the Dipartimento Geomineralogico (University of Bari, Italy). The authors would like to thank A.M. Karpoff and D.A.C. Manning for the constructive comments on the manuscripts, and F. Veniale and an anonymous for the review. B. Molloy has improved English language.

REFERENCES

ARTHUR M.A., JENKYNS H.C., BRUMSACK H.J. and SCHLANGER S.O. (1990) — *Stratigraphy, geochemistry and palaeogeography of organic carbon-rich Cretaceous sequences*. In: «Cretaceous Resources, Events and Rhythms» R.N. Ginsburg and B. Beaudoin (Eds.). Kluwer Academic, The Netherlands, 75-119.

BONARDI G., D'ARGENIO B. and PERRONE V. (1988) — *Carta geologica dell'Appennino meridionale alla scala 1:250.000. Breve presentazione*. Memorie Soc. Geol. It., **41**, 1341.

BOSTRÖM K., PETERSON M.N.A., JOENSUU O. and FISHER D.E. (1969) — *Aluminium poor ferromanganoan sediments on active oceanic ridges*. J. Gephys. Res., **74**, 3261-3270.

CALVERT S.E., BUSTIN R.M. and INGALL E.D. (1996) — *Influence of water column anoxia and sediment supply on the burial and preservation of organic carbon in marine shales*. Geochim. Cosmochim. Acta, **60**, 1577-1593.

CONDIE K.C. and WRONKIEWICZ D.J. (1990) — *The Cr/Th in Precambrian pelites from the Kaapvaal craton as an index of craton evolution*. Earth Planet. Sci. Lett., **97**, 256-267.

CULLERS R.L. (1994a) — *The chemical signature of source rocks in size fractions of Holocene stream sediment derived from metamorphic rocks in the Wet Mountains region, Colorado, USA*. Chem. Geol., **113**, 327-343.

CULLERS R.L. (1994b) — *The controls on the major and trace element variation of shales, siltstones, and sandstones of Pennsylvanian-Permian age from uplifted continental blockes in Colorado to platform sediment in Kansas, USA*. Geochim. Cosmochim. Acta, **58**, 4955-4972.

DILL H. (1986) — *Metallogenesis of early Palaeozoic graptolite shales from the Grafenthal Horst (northern Bavaria - Federal Republic of Germany)*. Econ. Geol., **81**, 889-903.

DYPVIK H. (1984) — *Geochemical compositions and*

depositional conditions of Upper Jurassic and Lower Cretaceous Yorkshire clays, England. Geol. Mag., **121**, 489-504.

EICHER D.L. and DINER R. (1991) — *Environmental factors controlling cretaceous limestone-marlstone rhythms.* In: «Cycles and Events in Stratigraphy» G. Einsele, W. Ricken and A. Seilacher (Eds.). Springer-Verlag, Berlin, 79-93.

FIORE S. and HUERTAS F.J. (1995) — *Rare earth, major, and trace elements in black shale levels from the Campomaggiore area (southern Italy).* In: *Proc. 8th Euroclay Conf.,* Leuven, Belgium, 416-417.

FRANZINI M., LEONI L. and SAITTA M. (1972) *A simple method to evaluate the matrix effects in X-ray fluorescence analysis.* X-Ray Spectrom., **1**, 151-154.

FRANZINI M., LEONI L. and SAITTA M. (1975) — *Revisione di una metodologia analitica per Fluorescenza-X, basata sulla correzione degli effetti di matrice.* Rend. Soc. Ital. Mineral. Petrol. **21**, 365-378.

GALLICCHIO S., MARCUCCI M., PIERI P., PREMOLI SILVA I., SABATO L., and SALVINI G. (1996) — *Stratigraphical data from a Cretaceous claystones sequence of the «Argille varicolori» in the Southern Apennine (Basilicata, Italy).* Palaeopelagos, **6**, 261-272.

JEFFERY P.J. (1970) — *Chemical methods of rock analysis.* Pergamon Press, Oxford.

JONES B. and MANNING D.A.C. (1994) — *Comparison of geochemical indices used for the interpretation of palaeoredox condition in ancient mudstones.* Chem. Geol., **111**, 111-129.

HARNOIS L. (1988) — *The CIW index: A new chemical index of weathering.* Sed. Geol., **55**, 319-322.

LEONI L. and SAITTA M. (1976) — *X-ray fluorescence analyses of 29 trace elements in rock and mineral standards.* Rend. Soc. Ital. Mineral. Petrol., **32**, 497-510.

MARCUCCI PASSERINI M., BETTINI P., DAINELLI J. and SIRUGO A. (1991) — *The «Bonarelli Horizon» in the central Apennines (Italy): radiolarian biostratigraphy.* Cret. Res., **12**, 321-331.

MCLENNAN S.M. (1989) — *Rare earth elements in sedimentary rocks: influence of provenance and sedimentary processes.* In «Geochemistry and Mineralogy of Rare Earth Elements». B.R. Lipin and G.A. McKay, (Eds.). Review in Mineralogy, 21, Mineralogical Society of America, Washington, 169-200.

MIDDELBURG J.J., VAN DER WEIJDEN C.H. and WOITTIEZ J.R.W. (1988) — *Chemical processes affecting the mobility of major, minor and trace elements during weathering of granitic rocks.* Chem. Geol., **68**, 253-273.

MIRABELLA A., CARNICELLI S. and CECCHINI G. (1993) — *Determinazione dei principali elementi presenti negli interstrati di vermiculiti «cloritizzate».* Annali Fac. Agr. Univ. di Sassari, **35**, 249-254.

MONGELLI G., CULLERS R.L. and MUELHEISEN S. (1996) — *Geochemistry of Late Cretaceous-Oligocenic shales from the Varicolori Formation, southern Apennines, Italy: implication for mineralogical, grain-size control and provenance.* Eur. J. Mineral., **8**, 733-754.

MOORE D.M. and REYNOLDS R.C. JR. (1989) — *X-Ray Diffraction and the Identification and Analysis of Clay Minerals.* Oxford University Press, NY.

MOSTARDINI F. and MERLINI S. (1986) — *Appennino centro-meridionale. Sezioni geologiche e proposta di modello strutturale.* Mem. Soc. Geol. It., **35**, 177-202.

MURRAY R.W. and LEINEN M. (1996) — *Scavenged excess aluminum and its relationship to bulk titanium in biogenic sediment from central equatorial Pacific Ocean.* Geochim. Cosmochim. Acta, **60**, 3869-3878.

OGNIBEN L. (1969) — *Schema introduttivo alla geologia del confine calabro-lucano.* Mem. Soc. Geol. It., **8**, 453-763.

OGNIBEN L. (1986) — *Relazione sul modello geodinamico «conservativo» della regione italiana.* ENEA spec. pub., Roma.

PEARCE T.H. and JARVIS I. (1992) — *Applications of geochemical data to modelling sediment dispersal patterns in distal turbidites: Late Quaternary of the Madeira Abyssal Plain.* J. Sed. Petrol., **62**, 1112-1129.

PESCATORE T., RENDA P. and TRAMUTOLI M. (1988) — *Rapporti tra le Unità Lagonegresi e le Unità Sicilidi nella media valle del Basento. Lucania (Appennino Meridionale).* Mem. Soc. Geol. It., **41**, 353-356.

PESCATORE T., RENDA P. and TRAMUTOLI M. (1992) — *«Tufiti di Tusa» e Flysch Numidico nella Lucania centrale (Appennino Meridionale).* Soc. Naz. Sci. Lett. Arti Napoli, **59**, 57-72.

PICKERING K.T., HISCOTT R.N. and HEIN F.J. (1989) — *Deep marine environments.* Unwin Hyman, London.

SCANDONE P. (1972) — *Studi di geologia lucana: nota illustrativa della carta dei terreni della serie calcareo-silico-marnosa.* Boll. Soc. Nat. Napoli, **81**, 225-300.

SCHULTZ L.G. (1964) — *Quantitative interpretation of mineralogical composition from X-ray and chemical data for the Pierre Shale.* U.S. Geol. Surv., Prof. Paper, **391-C**, 1-31.

SCHLANGER S.O. and JENKYNS P.A. (1976) —

Cretaceous oceanic anoxic events: causes and consequences. Geologie en Mijnbouw, **55**, 179-184.

SEIBOLD E. and BERGER W.H. (1996) — *The sea floor*. Springer-Verlag, Berlin.

SHAW D.B., STEVENSON R.G., WEAVER C.E. and BRADLEY W.F. (1971) — In «Procedures in Sedimentary Petrology» R.E. Carver. (Ed.). Wiley, New York, 554-557.

TAYLOR S.R. AND MCLENNAN S.M. (1985) — *The Continental Crust: Its Composition and Evolution*. Blackwell, Oxford.

VAN BENNEKOM A.J., JANSEN J.H.F., VAN DER GAAST S.J., VAN IPEREN J.M. and PIETERS J. (1989) — *Aluminium rich opal: an intermediate in the preservation of biogenic silica in Zaire (Congo) deep-sea fan*. Deep-Sea Res., **36**, 173-190.

VAN DE KAMP P.C. and LEAKE B.E. (1995) — *Petrology and geochemistry of siliciclastic rocks of mixed feldspathic and ophiolitic provenance in the Northern Apennines, Italy*. Chem. Geol., **122**, 1-20.

WAKITA H., REY P. and SCHMITT R.A. (1971) — *Abundance of the 14 rare-earth elements and 12 other trace-elements in Apollo 12 samples: five igneous and one breccia rocks and four soils*. In «Proc. 2nd Lunar Science Conf.», 1319-1329.

WILSON A.D. (1960) — *The micro-determination of ferrous iron in silicate minerals by a volumetric and a colorimetric method*. Analyst, **85**, 823-827.

WRONKIEWICZ D.J. and CONDIE K.C. (1989) — *Geochemistry and provenance of sediments from the Pongola Supergroup, South Africa: Evidence for a 3.0 Ga-old continental craton*. Geochim. Cosmochim. Acta, **53**, 1537-1549.

WRONKIEWICZ D.J. and CONDIE K.C. (1990) — *Geochemistry and mineralogy of sediments from the Webtersdorp and Traansval Supergroups, South Africa: cratonic evolution during the early Proterozoic*. Geochim. Cosmochim. Acta, **54**, 343-354.